

RESEARCH ARTICLE | MARCH 06 2024

Simple high-resolution Bradbury–Nielsen mass gate

Zezhao Jia; Zhaojun Liu; Xiaohan Wang; Runyu Wang ; Tianjie Ma ; Ziwen Zhou ; Ramiro Moro ; Bernd von Issendorff ; Lei Ma  



AIP Advances 14, 035312 (2024)

<https://doi.org/10.1063/5.0188688>



CrossMark

AIP Advances

Special Topic: Novel Applications of
Focused Ion Beams — Beyond Milling

Submit Today



Simple high-resolution Bradbury–Nielsen mass gate

Cite as: AIP Advances 14, 035312 (2024); doi: 10.1063/5.0188688

Submitted: 23 November 2023 • Accepted: 15 February 2024 •

Published Online: 6 March 2024



Ze Zhao Jia,¹ Zhaojun Liu,¹ Xiaohan Wang,¹ Runyu Wang,¹ Tianjie Ma,¹ Ziwen Zhou,¹ Ramiro Moro,¹ Bernd von Issendorff,² and Lei Ma^{1,a)}

AFFILIATIONS

¹Tianjin International Center for Nanoparticles and Nanosystems, Tianjin University, 92 Weijin Road, Nankai District, Tianjin 300072, People's Republic of China

²Physikalisches Institut, Universität Freiburg, H. Herderstr. 3., D-79104 Freiburg, Germany

^{a)}Author to whom correspondence should be addressed: lei.ma@tju.edu.cn

ABSTRACT

The selection of targets with specific masses, including molecules, atoms, and clusters, has broad applications in spectrometry. As an ion mass-gate with a very high resolution, Bradbury–Nielsen Gates (BNGs) are widely used in the study of size-dependent effects of clusters. Here, we present a simple and low-cost method for fabricating high resolution BNGs using a printed circuit board and a 3D printed wire winding and transfer tool. It can produce a pitch of 400 μm with 25 μm diameter tungsten wires. The test results indicate that its resolution reaches more than 1500 when it couples with a homemade ultrafast voltage switch.

© 2024 Author(s). All article content, except where otherwise noted, is licensed under a Creative Commons Attribution (CC BY) license (<http://creativecommons.org/licenses/by/4.0/>). <https://doi.org/10.1063/5.0188688>

I. INTRODUCTION

Mass selection is an essential prerequisite for the study of size effects in microscopic systems, such as nanoparticles and clusters. Known for high mass resolution, high ion transmittance, and rather low working voltage, Bradbury–Nielsen Gates (BNGs) have been widely used for ion mass selection in time-of-flight mass spectrometers since it was invented.^{1–9} Figure 1 shows the mode of operation of a BNG gate. A typical BNG consists of two sets of electrically isolated and uniformly stagger-spaced wires within a plane. When the same potential is applied, the BNG is highly transparent to the traversing ions, while when equal amplitude but opposite polarized voltages are applied to the two sets of wires, the charged particles will be scattered into two separate branches away from their original trajectories. Therefore, it is perfectly suitable to select the ions with specific masses in a time-of-flight mass spectrometer by properly setting the timing of gate closing and opening.

Weinkauff *et al.* installed a first BNG at the temporal focal point of a time-of-flight mass spectrometer and successfully realized particle mass selection, which starts the history of BNGs being used as ion

mass selectors.^{5,6,10–14} Later, Vlasak *et al.*⁸ proposed a design consisting of two sets of parallel tungsten wire arrays, which are mounted on two independent frames attached face to face so that the wires from the two frames are alternatively positioned with a spacing of 1 mm. Few years later, the spacing was further narrowed down to 0.5 mm using grooved nylon rods as positioners, but without placing the two sets of wires in the same plane.⁹ Further reducing the wire spacing to 0.16 mm was realized by placing wires manually in a silicon etched frame under a microscope, but it was an extremely tedious process that took several days to complete.^{3,15}

Kimmel *et al.* reported a machined polymer material based scheme to lower the line spacing to 0.075 mm, which required highly accurate machinery.¹⁶ In 2007, Zuleta *et al.* successfully fabricated a BNG on an insulating silicon wafer by micromachining, employing deep aspect ratio reactive ion etching. They realized a spacing of 25–100 μm on a 20 μm thick wafer and a $5 \times 5 \text{ mm}^2$ effective ion passage area.¹⁷ Although it reached an unprecedented line spacing, an extremely short transmission time, and a very high resolution, the complexity and cost of fabrication hinder its broader application. As an alternative, Du *et al.* proposed a PCB (printed circuit

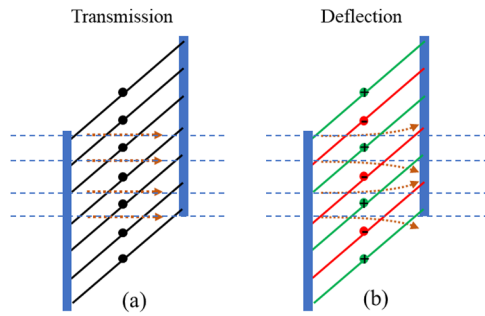


FIG. 1. Mode of operation of a BNG gate. (a) When the potentials on all wires are equal, ions can pass through the grid without deflection. (b) When there is a potential difference between the red and green wires, ions will deviate from the axial direction and be deflected in two directions.

broad) based design with a much lower complexity and cost in 2011; nevertheless, this proved not to be yet the optimal solution, as the uniformity of tension of the wires cannot be guaranteed, and the line spacing was 1 mm.¹⁸

In this work, we report a simple and reliable manufacturing method based on a 3D printed template. Compared with the traditional machining approaches, 3D printing is much more capable of producing complicated configurations at a lower cost due to reduced labor and material requirements.¹⁹ It has been widely used in making special parts, for example for applications in vacuum.²⁰ Here, 3D printing is used to produce auxiliary parts for a PCB frame based BNG mass gate, which greatly reduces the complexity of the tungsten wire winding process. The mass gate produced this way exhibits a very high transmission and mass selectivity.

II. DEVICE ASSEMBLY

A BNG is mainly composed of two groups of parallel wires. Figure 2 shows the manufacturing process of the PCB based BNG. The actual winding tool design is presented in Fig. S1. The design of BNG can be optimized through simulation.²¹

As shown in Fig. 2(a), a PCB board is used as the electrode substrate and device frame. The 2 mm long and 0.4 mm wide yellow and green stripes indicate the staggered aligned copper contact pads on the PCB board, which have a spacing of 0.8 mm. Each individual pad is connected by an embedded wire, and each group of electrodes is connected with the external circuit through pre-reserved solder joints.²² The physical design of the PCB board is shown in Figs. 3(a) and 3(b). The frame has an outer dimension of 40 mm with a 20 mm width inner square hole and a thickness of 1.6 mm. All wires are glued to the electrodes by silver paste; the solder joints have clearance holes of 0.2 mm diameter.

Figure 2(b) shows the winding process of parallel wires. A circular disk with a diameter of 100 mm is fixed on a bearing rod, and it is wrapped with a gold-plated tungsten wire with a diameter of 25 μm (providing good strength and conductivity). To ensure uniform spacing and sufficient tension to avoid wire kinking, one end of the tungsten wire is fixed on a 3D printed frame, while the other end is fixed to a 50 g weight. The disk is rotated to wind the tungsten wire onto the 3D printed frame with a sequence of 1 mm deep V-shaped grooves spaced equally with a distance of 400 μm . After the wire winding is complete, both sides of the parallel wires are fixed using cyanoacrylate, and the parallel wires on the backside are cut using scissors. Subsequently, the PCB frame was pushed against the wires, aligning with the contact pads, as shown in Fig. 2(c). Then, all wires are glued to the contact pads with silver paste [in Fig. 2(d)] and later using Torr Seal and a top ceramic cover for enforcement [in Fig. 2(e)]. Finally, after the Torr Seal cures, the wires protruding

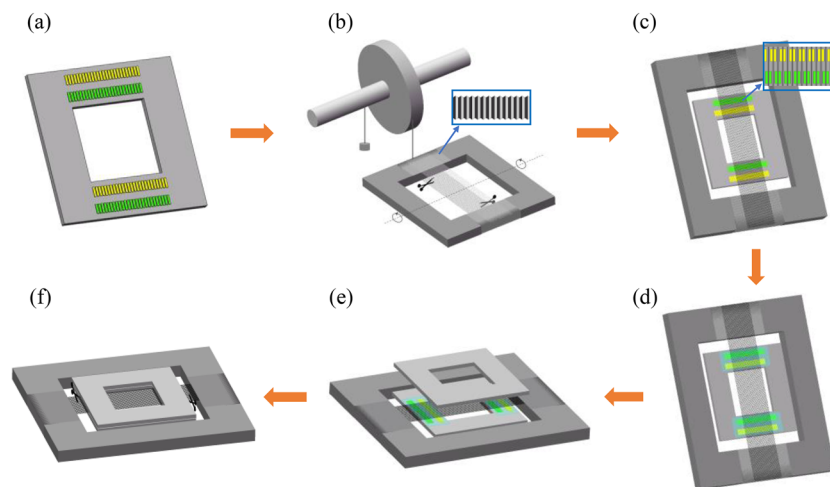


FIG. 2. Production of the BNG mass gate: (a) PCB board with contact pads; (b) wires wound around the 3D printed winding tool with evenly distributed grooves (with distances of 400 μm in this work); (c) alignment of the wires to the contact pads on the PCB; (d) wires are glued to the pads with silver paste; (e) wires are coated with a thin layer of Torr Seal and quickly covered with a ceramic plate; and (f) wires are cut, and the winding tool is removed (more detailed descriptions are presented in the supplementary material).

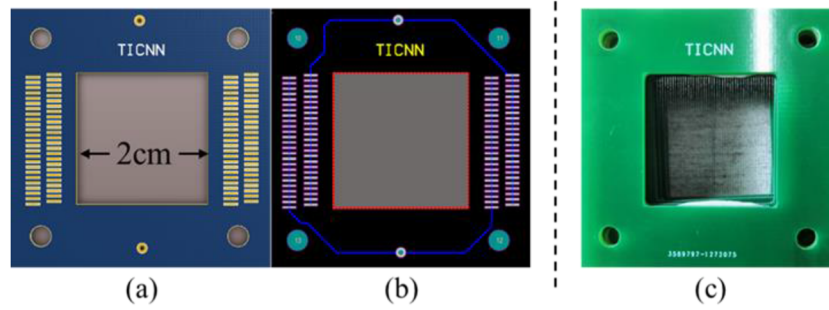


FIG. 3. (a) Photo of the PCB frame with contact pads. (b) Schematic of the PCB board showing the embedded wire connections. (c) Photo of the mass gate.

from the frame are removed with scissors, as shown in Fig. 2(f). The completed BNG is shown in Fig. 3(c).

III. EXPERIMENTAL TESTS

The performance of the BNG was tested in a time-of-flight mass spectrometer. Ions of a given mass are selected by applying pulsed voltages with opposite polarity to the wires of the BNG. The waveforms of the pulsed voltages are shown in Fig. 4. They have amplitudes of ± 100 V and rise and fall times of 8 and 13 ns, respectively. Here, a pulse width of 130 ns was used. Higher voltage pulses could deflect the ions to larger angles, but the unavoidable stronger ringing of such pulses and the larger spatial extension of the field could deteriorate the mass resolution. Therefore, the minimum voltage should be chosen, which reliably suppresses the transmission of the ions through the mass spectrometer. To justify the usage of 100 V, a voltage-dependent transmission rate of ions through the mass gate was measured and is shown in Fig. S2, which demonstrates that 100 V is sufficient enough to sweep away all ions that do not arrive with the right timing.

Figure 5(a) shows the simulated ion trajectories when ions are deflected by the BNG. As only ions that experience the electrical field get deflected, the key to realize a high resolution is to have a

switching time as short as possible and a spatial extension of the field as small as possible, which in turn is determined by the wire spacing.

The resolution of the BNG is, in fact, determined by the minimum length of an ion package it can cut out of a continuous ion beam as well as the spatial separation between ions of different masses at the position of the mass gate. The minimum ion package length depends on the effective range of the deflecting electric field along the direction normal to the wire plane as well as the rise and fall times of the field. The effective range of the electric field is numerically simulated by using the software package SIMION 8.1, as shown in Fig. 5(b); the rise and fall times of the pulses have been measured (Fig. 4). The effective ion separation can be obtained from the resolution of the time-of-flight spectrometer at the position of the mass gate and the effective flight path up to this point. The resolution R of the ion mass selection can then be roughly estimated by the following equation:

$$\frac{dm}{M} = \frac{1}{R} = \sqrt{\left(\frac{1}{R_0^2} + \frac{1}{R_l^2} + \frac{1}{R_t^2}\right)}, \quad (1)$$

where R_0 , $R_l = L/(2d)$, and $R_t = T/(2\tau)$ are the mass resolution of the time-of-flight mass spectrometer and the mass resolutions resulting from the spatial and temporal resolution of the BNG, respectively.

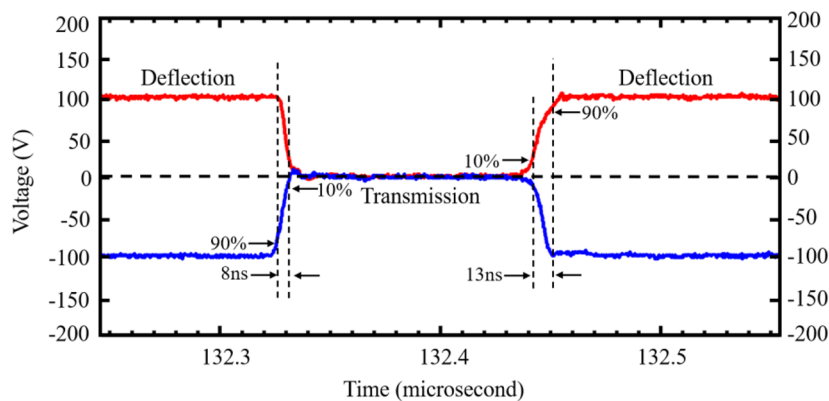


FIG. 4. Electrical pulses applied to the mass gate wires. The rise and fall times of the pulses are 8 and 13 ns, respectively.

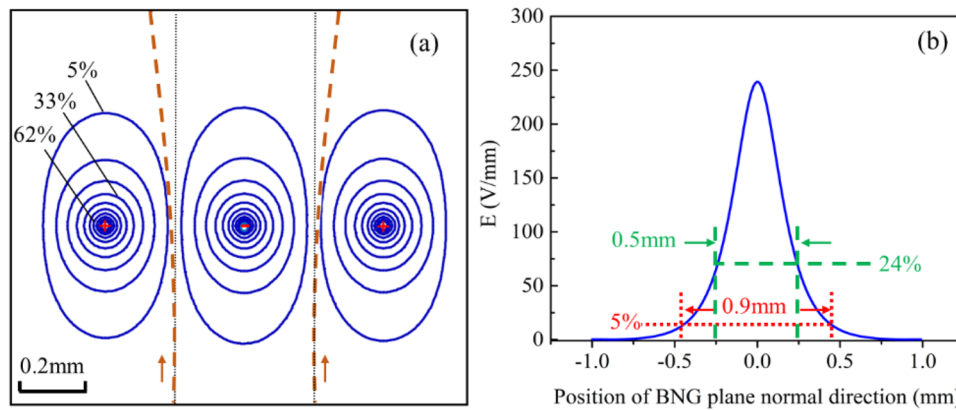


FIG. 5. (a) Simulated ion trajectories of negative ions deflected by the BNG with alternating voltages applied to the wires. The ion kinetic energy here is 1100 eV, and the applied voltage is ± 100 V. Simulations were done using SIMION.^{23,24} (b) Simulated electric field strength along a line perpendicular to the BNG plane and centered between two adjacent wires. The effective range of the field is defined as the length where the field strength is larger than 5% of the maximum value.

This rough estimate is based on the idea that the resolution R of BNG is limited by the combined effects of error from the factors R_0 , R_i , and R_t . T is the arrival time of the ions at the BNG, and $L = T \times v$ is the effective flight path (v : ion velocity). The minimum possible ion package length of heavy (slow) ions has been set equal to the wire spacing d , and the minimum temporal package length of light (fast) ions has been set equal to the rise or fall time τ . In our case, the wire spacing is $d = 400 \mu\text{m}$, the rise/fall time is about 10 ns, and the mass resolution of the mass spectrometer at the point of the mass gate is about $R_0 = 2500$, with an effective flight path L up to the BNG of 3 m.

As an example, for an ion with a mass of 371.6 amu (Nb_4^+) and a kinetic energy of 1100 eV (resulting in a velocity of $v = 23\,815$ m/s), the mass resolution resulting from the spatial and temporal characteristics of the BNG would then be $R_i = 3750$ and $R_t = 6298.5$, resulting in an overall resolution of $R = 1975$. This shows that for ions of this mass, the resolution of the BNG is mainly determined

by the resolution of the mass spectrometer and the wire spacing in relation to the total effective flight path up to the mass gate; for much faster ions, the switching time will become the decisive parameter.

To characterize the performance of the BNG as a mass gate, it was installed at the first temporal focal point of a double-reflectron type time-of-flight mass spectrometer, with the above-mentioned characteristics. Scanning the timing of the pulses while monitoring the intensity of a certain ion (here Nb_4^+) was used to determine the resolution of the BNG. The time interval changes corresponding to a signal increase from 10% to 90% (or decrease from 90% to 10%) of the maximum value is defined as Δt . As shown in Fig. 6, the measured Δt is 44 and 39 ns by using the above two ways, respectively. The corresponding mass resolution of the onset and end of the ion beam deflection is then given by $T/(2 \times \Delta t)$. This results in a FWHM of a minimum width ion package, which also corresponds to a resolution of about $R = T/(2 \times \Delta t)$.

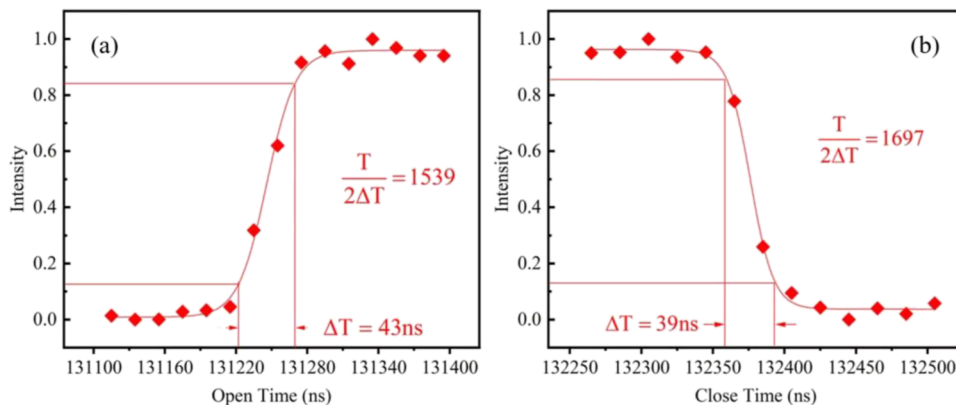


FIG. 6. (a) and (b) Measured Nb_4^+ intensity change with the timing of firing and shut-down pulses, respectively, which corresponds to the timing of opening and closing mass gate.

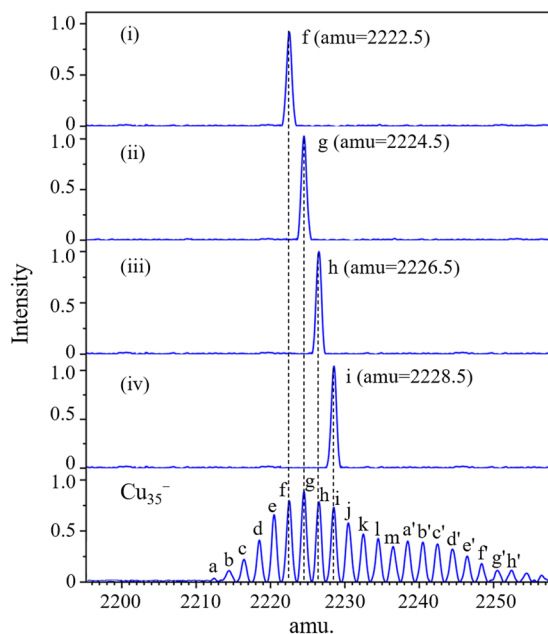


FIG. 7. Mass spectra of Cu_{35}^- , where a–m are isotope peak of Cu_{35}^- and a'–h' are isotope peak of Cu_{35}O^- . (i)–(iv) Spectra after mass selection of Cu_{35}^- peak f (2222.5 amu), peak g (2224.5 amu), peak h (2226.5 amu), and peak i (2228.5 amu), respectively.

Figure 7 finally demonstrates the selection of single masses out of the broad isotope distribution of Cu_{35}^- clusters. For the selection of a single mass in this mass range, a resolution of at least $R = 1111$ is needed; the very good suppression of neighboring masses indicates an even better resolution.

IV. CONCLUSIONS

We have presented a simple and low-cost scheme to manufacture a PCB electrode based BNG. A 3D printed winding die is employed for the wire winding process, which results in precise wire spacing and uniform wire tension. Adopting a PCB provides a reliable method for contacting the wires and together with a ceramic cover a rather sturdy packaging of the setup. Using such a BNG with 400 μm wire spacing in an existing time-of-flight mass spectrometer led to a mass selectivity with a resolution of at least 1500, indicating that this mass gate can produce ion pulses with a spatial extension of less than 1 mm.

SUPPLEMENTARY MATERIAL

See the supplementary material for a description of the winding process and a schematic diagram of the winding device, a detailed description of BNG fabrication, and an experimental test relationship between the pulse voltage applied to the mass gate and the ion intensity.

ACKNOWLEDGMENTS

This work was supported by the National Key R&D Program of China under Grant No. 2020YFC2004602.

AUTHOR DECLARATIONS

Conflict of Interest

The authors have no conflicts to disclose.

Author Contributions

Z.J. and Z.L. contributed equally to this work.

Zezhao Jia: Data curation (equal); Validation (equal); Writing – original draft (equal). **Zhaojun Liu:** Data curation (equal); Investigation (equal). **Xiaohan Wang:** Data curation (equal); Methodology (equal). **Runyu Wang:** Data curation (equal); Validation (equal). **Tianjie Ma:** Data curation (equal); Investigation (equal). **Ziwen Zhou:** Data curation (equal); Investigation (equal). **Ramiro Moro:** Writing – review & editing (equal). **Bernd von Issendorff:** Formal analysis (equal); Writing – review & editing (equal). **Lei Ma:** Conceptualization (equal); Formal analysis (equal); Funding acquisition (equal); Investigation (equal); Methodology (equal); Supervision (equal); Writing – review & editing (equal).

DATA AVAILABILITY

The data that support the findings of this study are available from the corresponding author upon reasonable request.

REFERENCES

- O.K. Yoon, I.A. Zuleta, M.D. Robbins, G.K. Barbula, and R.N. Zare, “Simple template-based method to produce Bradbury-Nielsen gates,” *J. Am. Soc. Mass Spectrom.* **18**, 1901 (2007).
- T. Dickel, P.J. Lang, J. Ebert, H. Geissel, E. Haettner, C. Jesch, W. Lippert, M. Petrick, and C. Scheidenberger, “Multiple-reflection time-of-flight mass spectrometry for in situ applications,” *Nucl. Instrum. Methods. Phys. Res. B* **317**, 779 (2013).
- A. Brock, N. Rodriguez, and R. N. Zare, “Characterization of a Hadamard transform time-of-flight mass spectrometer,” *Rev. Sci. Instrum.* **71**, 1306 (2000).
- X. M. Qian, T. Zhang, C. Chang, P. Wang, C. Ng, Y.-H. Chiu, D. J. Levandier, J. S. Miller, R. A. Dressler, T. Baer, and D. S. Peterka, “High-resolution state-selected ion-molecule reaction studies using pulsed field ionization photoelectron-secondary ion coincidence method,” *Rev. Sci. Instrum.* **74**, 4096 (2003).
- R. Weinkauff, K. Walter, C. Weickhardt, U. Boesl, and E. Schlag, “Laser tandem mass spectrometry in a time of flight instrument,” *Z. Naturforsch. A* **44**, 1219 (1989).
- D. J. Beussman, P. R. Vlasak, R. D. McLane, M. A. Seeterlin, and C. G. Enke, “Tandem reflectron time-of-flight mass spectrometer utilizing photodissociation,” *Anal. Chem.* **67**, 3952 (1995).
- A. Brock, N. Rodriguez, and R. N. Zare, “Hadamard transform time-of-flight mass spectrometry,” *Anal. Chem.* **70**, 3735 (1998).
- P. R. Vlasak, D. J. Beussman, M. R. Davenport, and C. G. Enke, “An interleaved comb ion deflection gate for m/z selection in time-of-flight mass spectrometry,” *Rev. Sci. Instrum.* **67**, 68 (1996).
- C. W. Stoermer, S. Gilb, J. Friedrich, D. Schooss, and M. M. Kappes, “A high resolution dual mass gate for ion separation in laser desorption/ionization time of flight mass spectrometry,” *Rev. Sci. Instrum.* **69**, 1661 (1998).

- ¹⁰T. Brunner, A. R. Mueller, K. O'sullivan, M. C. Simon, M. Kossick, S. Ettenauer, A. T. Gallant, E. Mané, D. Bishop, M. Good *et al.*, "A large Bradbury Nielsen ion gate with flexible wire spacing based on photo-etched stainless steel grids and its characterization applying symmetric and asymmetric potentials," *Int. J. Mass Spectrom.* **309**, 97 (2012).
- ¹¹Y. Du, W. Wang, and H. Li, "Bradbury-Nielsen-gate-grid structure for further enhancing the resolution of ion mobility spectrometry," *Anal. Chem.* **84**, 5700 (2012).
- ¹²K. Guo, C. Zhang, K. Ni, and X. Wang, "Modeling the modulation characteristics of the Bradbury-Nielsen gate in ion mobility spectrometers," *Rev. Sci. Instrum.* **93**, 084101 (2022).
- ¹³J. Puton, A. Knap, and B. Siodłowski, "Modelling of penetration of ions through a shutter grid in ion mobility spectrometers," *Sens. Actuators, B* **135**, 116 (2008).
- ¹⁴A. W. Szumlas, D. A. Rogers, and G. M. Hieftje, "Design and construction of a mechanically simple, interdigitated-wire ion gate," *Rev. Sci. Instrum.* **76**, 086108 (2005).
- ¹⁵N. Rodriguez, *Hadamard Transform Time-of-Flight Mass Spectrometry: Implementation and Characteristics* (Stanford University, 2000).
- ¹⁶J. R. Kimmel, F. Engelke, and R. N. Zare, "Novel method for the production of finely spaced Bradbury-Nielsen gates," *Rev. Sci. Instrum.* **72**, 4354 (2001).
- ¹⁷I. A. Zuleta, G. K. Barbula, M. D. Robbins, O. K. Yoon, and R. N. Zare, "Micromachined Bradbury-Nielsen gates," *Anal. Chem.* **79**, 9160 (2007).
- ¹⁸Y. Z. Du, H. W. Cang, W. G. Wang, F. Han, C. Chen, L. Li, K. Hou, and H. Li, "Note: Design and construction of a simple and reliable printed circuit board-substrate Bradbury-Nielsen gate for ion mobility spectrometry," *Rev. Sci. Instrum.* **82**, 086103 (2011).
- ¹⁹A. Ramya and S. L. Vanapalli, "3D printing technologies in various applications," *Int. J. Mech. Eng. Technol* **7**, 396 (2016).
- ²⁰S. D. S. Gordon and A. Osterwalder, "3D-printed beam splitter for polar neutral molecules," *Phys. Rev. Appl.* **7**, 044022 (2017).
- ²¹M. Salleras, A. Kalms, A. Krenkow, M. Kessler, J. Goebel, G. Müller, and S. Marco, "Electrostatic shutter design for a miniaturized ion mobility spectrometer," *Sens. Actuators, B* **118**, 338 (2006).
- ²²N. Kai, G. Jingran, O. Guangli, L. Yu, Y. Quan, Q. Xiang, and W. Xiaohao, "A simple template-based transfer method to fabricate Bradbury-Nielsen gates with uniform tension for ion mobility spectrometry," *Rev. Sci. Instrum.* **85**, 085107 (2014).
- ²³D. Manura and D. Dahl, SIMION (R) 8.1 User Manual, Adaptas Solutions LLC, Palmer, MA, 2008.
- ²⁴D. A. Dahl, J. E. Delmore, and A. D. Appelhans, "SIMION PC/PS2 electrostatic lens design program," *Rev. Sci. Instrum.* **61**, 607 (1990).